Resolution of the conformational distribution and dynamics of a flexible molecule using frequency-domain fluorometry

ARTICLE *in* BIOPHYSICAL CHEMISTRY · FEBRUARY 1991

Impact Factor: 1.99 · DOI: 10.1016/0301-4622(91)85008-E · Source: PubMed

Biophysical Chemistry, 39 (1991) 79–84
Elsevier

BIOCHE 01530

Resolution of the conformational distribution and dynamics of a flexible molecule using frequency-domain fluorometry

Joseph R. Lakowicz [a], Józef Kuśba [a,*], Wieslaw Wiczk [a], Ignacy Gryczynski [a], Henryk Szmacinski [a] and Michael L. Johnson [b]

[a] *University of Maryland, School of Medicine, Center for Fluorescence Spectroscopy, Department of Biological Chemistry, 660 West Redwood Street, Baltimore, MD 21201 and* [b] *University of Virginia, Department of Pharmacology, Charlottesville, VA 22908, U.S.A.*

Received 31 July 1990
Revised manuscript received 7 August 1990
Accepted 7 August 1990

Fluorescence; Molecular dynamics; Conformational analysis; Resonance energy transfer; Frequency-domain fluorometry

We report the first resolution of both the conformational distribution and end-to-end diffusion coefficient of a flexible molecule. This molecular information was recovered using only the donor intensity decay in a single solvent at a single viscosity, as observed by the technique of frequency-domain fluorometry. This technique can be extended to measurements of structural fluctuations of biological macromolecules.

1. Introduction

The function of proteins, membranes and other biomolecules depends on their conformation and dynamics [1,2]. Fluorescence spectroscopy, with its high sensitivity and natural time-window on the pico- to nanosecond time scale, makes this technique the method of choice for studies of biopolymer dynamics [3–7]. However, obtaining useful information from the emission requires high-resolution measurements of the complex fluorescence intensity or anisotropy decays. Such resolution has recently become available using the frequency-domain method [8–10].

In this preliminary report, we used the phenomenon of fluorescence resonance (nonradiative) energy transfer (FRET) [11] to recover both the end-to-end distance distribution and diffusion coefficients of a flexible molecule (TUD; fig. 1). FRET occurs from the tryptamine donor to the dansyl acceptor. A previous publication [12] claims that time-domain measurements of the donor emission alone are inadequate to resolve both the initial $t = 0$ distance distribution and the end-to-end diffusion coefficient. However, the results of the present paper demonstrate that the frequency response of the donor emission alone is easily capable of determining these static and dynamic molecular characteristics.

2. Theory

Consider a flexible molecule described by a Gaussian end-to-end distance (r) probability distribution

$$N_0(r) = \frac{1}{\sigma\sqrt{2\pi}} \exp\left[-\left(\frac{r - R_{av}}{2\sigma}\right)\right]^2 \qquad (1)$$

Correspondence address: J.R. Lakowicz, University of Maryland, School of Medicine, Center for Fluorescence Spectroscopy, Department of Biological Chemistry, 660 West Redwood Street, Baltimore, MD 21201, U.S.A.

* Permanent address: Technical University of Gdańsk, Department of Technical Physics, 80-952 Gdańsk, Poland.

where R_{av} is the mean distance and the half-width (hw) of the distribution is given by $hw = \sigma\sqrt{8 \cdot \ln 2}$. Assume that the molecule undergoes end-to-end diffusion characterized by a diffusion coefficient D. According to ref. 13, the time-dependent change in concentration $N^*(r,t)$ of excited donor molecules with the end-to-end distance r is described by the diffusion equation with an additional distance-dependent transfer term,

$$\frac{\partial \bar{N}^*(r,t)}{\partial t} = -\frac{1}{\tau}\left[1 + \left(\frac{R_0}{r}\right)^6\right]\bar{N}^*(r,t) + \frac{1}{N_0(r)} \times \frac{\partial}{\partial r}\left[N_0(r) D \frac{\partial \bar{N}^*(r,t)}{\partial r}\right] \quad (2)$$

In this expression $N_0(r)$ denotes the initial donor-to-acceptor distance distribution (at $t = 0$) of the excited molecules, $\bar{N}^*(r,t) = N^*(r,t)/N_0(r)$ is the excitation probability normalized by the $t = 0$ distance distribution, τ is the donor fluorescence lifetime in the absence of an acceptor, and R_0 is the critical distance for donor-acceptor energy transfer. The initial condition is $\bar{N}^*(r, t = 0) = 1$. At each distance r the rate (k_T) of donor-to-acceptor transfer is $k_T = \tau^{-1}(R_0/r)^6$ [11]. The first term on the right describes depletion of the excited donor population due to spontaneous emission and nonradiative energy transfer. The rightmost term described repopulation of the excited donor population by end-to-end diffusion.

To recover the donor distribution and diffusion parameters, eq. 2 is solved with appropriate boundary conditions. We assumed that, apart from the long-range energy transfer, there is no additional reaction between excited donors and acceptors, either at the encounter distance r_{min} or at the maximal distance r_{max}. Hence, we used the reflecting boundary correlations at r_{min} and r_{max}

$$\left[\frac{d\bar{N}^*(r,t)}{dr}\right]_{r=r_{min}} = 0 \quad (3)$$

$$\left[\frac{d\bar{N}^*(r,t)}{dr}\right]_{r=r_{max}} = 0 \quad (4)$$

In this work we used an algorithm which is analogous to that described in ref. 14. This method involves solution of eq. 2 in Laplace space [15], followed by inversion to time [16], and then least-square fitting of the Fourier transform to the experimental data [17,18].

The frequency-domain data were also analyzed using the multi-exponential model,

$$I(t) = \sum_i \alpha_i e^{-t/\tau_i} \quad (5)$$

where α_i are the pre-exponential factors and τ_i the decay times [9,18]. The fractional intensity of each component in the decay is given by

$$f_i = \frac{\alpha_i \tau_i}{\sum_j \alpha_j \tau_j} \quad (6)$$

The goodness-of-fit is characterized by

$$\chi^2_R = \frac{1}{\nu}\sum_\omega \left[\frac{\phi_\omega - \phi_{c\omega}}{\delta\phi}\right]^2 + \frac{1}{\nu}\sum_\omega \left[\frac{m_\omega - m_{c\omega}}{\delta m}\right]^2 \quad (7)$$

where ν is the number of degrees of freedom, and $\delta\phi$ and δm are the experimental uncertainties in the measured phase angles (ϕ_ω) and modulation (m_ω), respectively.

3. Materials and methods

Syntheses of the donor control (TMA) and donor-acceptor pair (TUD) are described in ref. 19. Also described in ref. 19 is the value of $R_0 =$ 25.7 Å in propylene glycol at 5 °C, the frequency-domain measurements in this solvent, and the distance distribution. Frequency-domain measurements were performed on the instrument described previously in detail [10]. All intensity decays were measured by using rotation-free polarization conditions, 290 nm excitation, with the donor emission selected by a 360 nm interference filter, 10 nm bandwidth, in methanol at 20 °C. Under these conditions, the Förster distance was found to be 24.9 Å as determined from the quantum yield and spectral overlap. For all analyses the uncertainties in the phase ($\delta\phi$) and modulation (δm) values were taken as 0.2° and 0.005, respectively.

4. Results

Emission spectra and structures of the donor alone (TMA) and of the donor-acceptor pair are shown in fig. 1. The donor emission centered at 355 nm is quenched by the presence of a covalently linked acceptor. The extent of quenching is greater in the nonviscous solvent methanol (20 °C, continuous line) than in the more viscous solvent propylene glycol (5 °C, broken line). The increased quenching in methanol is due to end-to-end diffusion which occurs during the donor decay time in methanol, but which is too slow in the more viscous solvent.

The frequency response (●) of the donor emission in methanol is shown in fig. 2. Also shown is the best fit to the data using eq. 2. This fit results in a diffusion coefficient of 2.6×10^{-6} cm^2/s (26 Å^2/ns) and a $t = 0$ distance distribution (fig. 3) which is nearly identical to that found in propylene glycol [19] where diffusion is not significant during the excited-state lifetime. Also shown in fig. 2 is the frequency response expected for a static distance distribution (------), with the same distance distribution as shown in fig. 3. This illustrates the substantial contribution of diffusion to the time-dependent donor emission. The shift towards higher frequencies is the result of the shorter donor decay resulting from end-to-end diffusion.

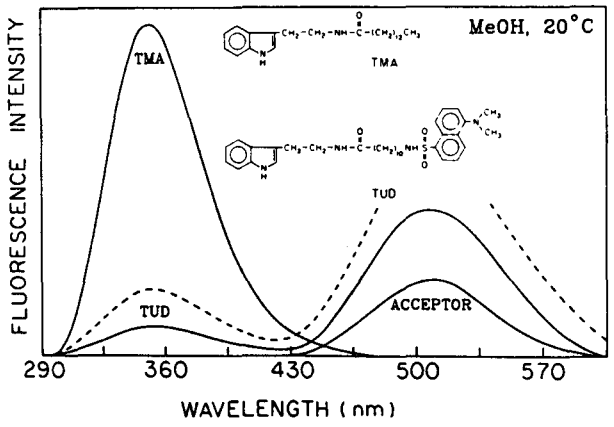

Fig. 1. Emission spectra of the donor alone (TMA), acceptor alone (dansyl amide) and of the donor-acceptor pair (TUD) in methanol at 20 °C (———) and in propylene glycol at 5 °C (------).

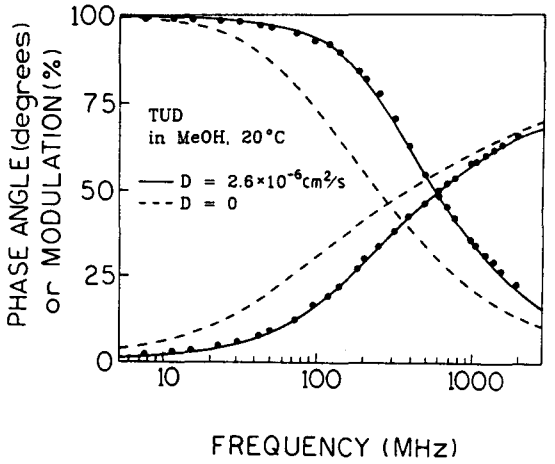

Fig. 2. Frequency response of the donor emission. The dots (●) are the experimental data, the solid line the best fit with $D = 2.6 \times 10^{-6}$ cm^2/s, $R_{av} = 12.2$ Å and hw = 13.0 Å, and the dashed line is the frequency-response expected for the distance distribution in fig. 3 with no diffusion ($D = 0$).

The results of the donor intensity decay analyses are summarized in table 1. The donor alone (TMA) shows a single-exponential decay, as indicated by $\chi_R^2 = 1.6$. A single-exponential decay for the donor is not a requirement of our analysis method, which has been extended to multi-exponential donors [20,21]. The presence of the acceptor in TUD results in a complex donor decay which cannot be fitted by a single decay time ($\chi_R^2 = 491$) and requires at least three decay times for a satisfactory fit. This effect is due to the presence of acceptor at a range of distances from the donor. However, the data are accounted for by the diffusive model (eq. 2). We note that the data cannot be fitted if one assumes that the donor and acceptor are at a

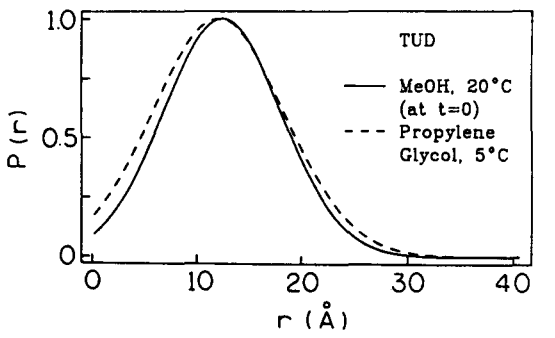

Fig. 3. Distance distributions for TUD in methanol at 20 °C (———) and in propylene glycol at 5 °C (------) [19].

Table 1

Donor decay analysis for the TMA donor and the TUD donor-acceptor pair in methanol at 20 °C

Compound	τ_i (ns)	α_i	R_{av} (Å)	hw (Å)	D ($\times 10^6$)(cm^2/s)	χ^2_R
TMA	5.76	1.0	–	–	–	1.61
TUD	0.35	1.0	–	–	–	491.0
	0.11	0.57	–	–	–	–
	0.57	0.43	–	–	–	3.9
	0.04	0.73	–	–	–	–
	0.16	0.14	–	–	–	–
	0.60	0.13	–	–	–	1.9
TUD	–	–	12.2	13.0	2.6	2.3
	–	–	15.8	⟨1⟩ [a]	0.063	387.5
	–	–	14.6	5.7	⟨0⟩	19.6

[a] The angular brackets ⟨ ⟩ indicate this parameter was held fixed at the indicated value.

single distance, i.e., a narrow distance distribution (hw = 1 Å), even with a floating mean distance and diffusion coefficient ($\chi^2_R = 388$). This result indicates that the data contain significant information on the $t = 0$ distance distribution. Additionally, the data cannot be fitted (table 1) if the diffusion coefficient is set to zero ($\chi^2_R = 19.6$), indicating that the data are not consistent with any static distance distribution. These results demonstrate that we were able to recover both the end-to-end distance distribution and diffusion coefficient from the frequency-domain data of the donor decay.

It is of interest to consider the range of distance distribution parameters and diffusion coefficients which are consistent with our experimental data. This uncertainty analysis is of particular interest given the suggestion [12] that correlation between the parameters prevents resolution of the type shown in figs 2 and 3. Consequently, we examined the χ^2_R surfaces for R_{av}, hw and D (fig. 4). Such surfaces account for all correlations because the minimum value of χ^2_R is calculated for each fixed parameter on the x-axis. The intersection of these surfaces with the 67% F-statistics (------) can be taken as the range of values consistent with the data, and from experience we know that this procedure overestimates the uncertainties by at least 50%. Hence, the χ^2_R surfaces in fig. 4 demonstrate that R_{av}, hw and D are determined from the donor-alone frequency response. Importantly, the range of values is modest, and there are no local minimum and/or flat regions in χ^2_R which could result in poorly determined parameters and/or nonconvergent fits. It should be emphasized that such resolution is only to be expected if the decay times and diffusion rates are comparable in magnitude.

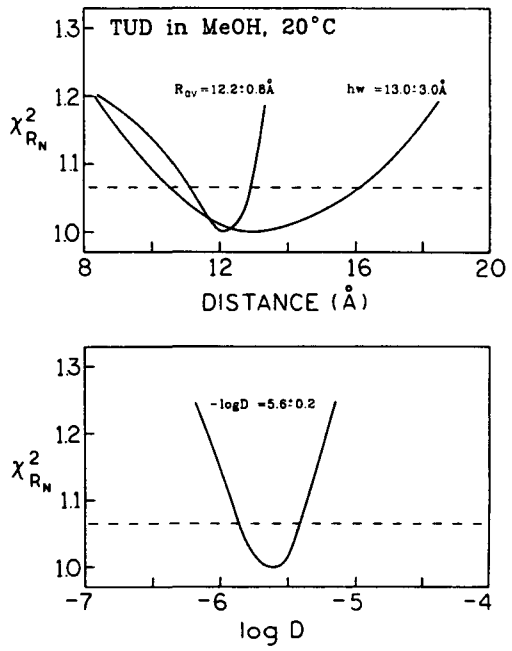

Fig. 4. Distance distribution and diffusion coefficient χ^2_R surfaces for TUD in methanol at 20 °C.

5. Discussion

Why were we able to recover both the end-to-end diffusion coefficient and distance distribution when the simulations by Beechem and Haas [12] suggested that such resolution was not possible? One possible reason for this apparent discrepancy is due to the use of different methods. Beechem and Haas simulated time-domain data with a limited number of counts (20000 counts) in the peak channel. In contrast, we used frequency-domain measurements, which resulted in distance distribution and diffusion-χ^2_R surfaces using the donor-alone data which are vastly superior to those presented by Beechem and Haas [12] for the donor-alone data.

Beechem and Haas [12] also claimed that resolution of the distance distribution and diffusion was only possible using global analysis of data for both the donor and the acceptor. In our opinion the value of the acceptor decay data is overestimated in their analysis. Specifically, the authors appear to assume that all the acceptor emission results from energy transfer from the donor. In almost every experimental situation excitation of the donor also results in excitation of the acceptor due to the longer absorption wavelengths of the acceptors. The directly excited acceptors are often the dominant origin of the acceptor emission when one excites a covalently linked donor-acceptor pair at the absorption maximum of the donor. Consequently, a significant if not dominant fraction of the acceptor emission results from directly excited acceptors, and this acceptor emission does not contain information on the distance distribution or diffusion coefficient. Hence, actual experimental data for the acceptor will provide less information than predicted by Beechem and Haas [12]. We note that their formalism appears to contain the ability to account for directly excited acceptors (their eq. 5), but this effect was apparently not included in their simulations.

Our experimental methods and analysis described above can be readily extended to biological macromolecules. For instance, it should be possible to recover end-to-end distances and diffusion rates for labeled proteins [21,22], nucleic acids [23] and lipids [24]. Such data can provide a more detailed view of the solution dynamics of macromolecules, which can be used to correlate biological dynamics with function or for comparison of theoretical calculations of dynamics.

Acknowledgements

The work was supported by Grants GM 35154 from the NIH and DMB 8804939 from the NSF, with support for instrumentation from NSF Grant DIR 8710401 and DMB 8502835. J.R.L. and W.W. acknowledge support from the Medical Biotechnology Center of the University of Maryland and J.K. would like to acknowledge the Kosciuszko Foundation in New York for fellowship support which contributed to this research and the Polish Academy of Sciences for partial financial help within the program CPBP 01.06.

References

1 J.A. McCammon and S.C. Harvey, Dynamics of proteins and nucleic acids (Cambridge University Press, New York, 1987).
2 G.R. Welch, The fluctuating enzyme (Wiley, New York, 1986).
3 E. Clementi, G. Corongui, M.H. Sarma and R.H. Sarma, Structure and motion: Membranes, nucleic acids and proteins (Adenine Press, New York, 1985).
4 A.P. Demchenko, Ultraviolet spectroscopy of proteins (Springer, New York, 1987).
5 A.R. Holzwarth, Q. Rev. Biophys. 22 (1989) 239.
6 D.M. Jameson and G.D. Reinhart, Fluorescence biomolecules (Plenum, New York, 1989).
7 J.R. Lakowicz, Time-resolved laser spectroscopy in biochemistry II, SPIE 1204, 1-850, (Bellingham, Washington, 1990).
8 E. Gratton and M. Limkeman, Biophys. J. 44 (1983) 315.
9 J.R. Lakowicz and B.P. Maliwal, Biophys. Chem. 21 (1985) 61.
10 J.R. Lakowicz, G. Laczko and I. Gryczynski, Rev. Sci. Instrum. 57 (1986) 2499.
11 T. Förster, Ann. Phys. (Leipzig) 2 (1948) 55 (Translated by R.S. Knox).
12 J.M. Beechem and E. Haas, Biophys. J. 49 (1989) 1225.
13 E. Haas, E. Katchalski-Katzir and I. Steinberg, Biopolymers 17 (1978) 11.
14 J. Kuśba, J. Luminescence 37 (1987) 287.
15 L. Fox, Proc. Roy. Soc. Lond. A190 (1947) 31.
16 H. Stehfest, Commun. ACM 13 (1970) 47.

17 J.R. Lakowicz, J. Kuśba, W. Wiczk, I. Gryczynski and M.L. Johnson, Chem. Phys. Lett. (1990) in the press.
18 J.R. Lakowicz, E. Gratton, G. Laczko, H. Cherek and M. Limkeman, Biophys. J. 46 (1984) 463.
19 J.R. Lakowicz, M.L. Johnson, W. Wiczk, A. Bhat and R.F. Steiner, Chem. Phys. Lett. 138 (1987) 587.
20 J.R. Lakowicz, I. Gryczynski, H.C. Cheung, C. Wang and M.L. Johnson, Biopolymers 27 (1988) 821.
21 J.R. Lakowicz, I. Gryczynski, H.C. Cheung, M.L. Johnson and N. Joshi, Biochemistry 27 (1988) 9149.
22 J.R. Lakowicz, W. Wiczk, I. Gryczynski, H. Szmacinski and M.L. Johnson, Biophys. Chem. 38 (1990) 89.
23 A.I.H. Murchie, R.M. Clegg, E. von Kitzing, D.R. Duckett, S. Diekmann and D.M.J. Lilley, Nature 341 (1989) 763.
24 T.S. Squier, W. Wiczk, M.L. Johnson and J.R. Lakowicz, in preparation.